First results of systematic studies done with Silicon Photomultipliers

C. Bosio [a] S. Gentile [b] E. Kuznetsova [a,*] F. Meddi [b]

[a] *INFN Roma 1,Piazzale Aldo Moro 5 00185 Roma, Italy*

[b] *Università degli Studi di Roma "La Sapienza", Piazzale Aldo Moro 5 00185 Roma, Italy*

Abstract

Multicell avalanche photodiode structure operated in Geiger mode usually referred as silicon photomultiplier is a new intensively developing technology for light detection. The insensitivity to magnetic fields, low operation voltage and small size make silicon photomultipliers very attractive for high-energy physics, astrophysics and medical applications.

The presented results are obtained during the first steps taken in order to develop a setup and measurement procedures which allow to compare properties of diverse samples of silicon photomultipliers available on market. The response to low-intensity light was studied for silicon photomultipliers produced by CPTA (Russia), Hamamatsu (Japan), ITC-irst (Italy) and SensL (Ireland).

Key words: silicon photomultipliers, photon detection
PACS: 29.40.Wk

1. Introduction

Silicon photomultiplier is a novel type of photodetectors with a multicell photodiode structure operating in the limited Geiger mode. The technology development started in 90's [1],[2] provided the photodetectors with a single photoelectron gain of about 10^6 and photodetection efficiency comparable with the one of vacuum photomultipliers. The same time the small size, capability to operate in a magnetic field, low bias voltage and reasonable price of the device induced a further intense development and enhancement of the technology leaded by different institutions and manufacturers. This results in a number of different types of silicon photomultipliers available on market and produced by different manufacturers. Despite the different commercial name of the devices here they are referred as SiPM.

Systematic studies done with various types of SiPM would provide start information for an optimal choice of the device appropriate for a given application. The results presented here are obtained during the first steps taken in order to develop a setup and measurement procedures which allow to compare properties of diverse SiPM samples.

2. General principle of the SiPM operation

The SiPM consist of large number of identical microcells with a common anode. The microcells are located on a common substrate with typical size of $\sim 1 \times 1$ mm^2. Fig. 1 shows a schematic view of a SiPM microcells.

Under the reverse bias voltage above the breakdown, the multilayer structure with a different doping concentrations provides high gradient of the electric field in vicinity of the np-junction region. The electrons created via photo-absorption in the π-region drift toward the p layer where the avalanche multiplication occurs. The resistive layer on the top

* Corresponding author.
Email address: Ekaterina.Kouznetsova@roma1.infn.it (E. Kuznetsova).

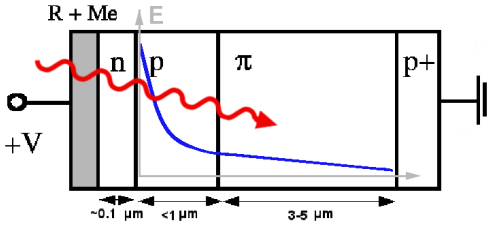

Fig. 1. The schematic view of a SiPM microcell.

of the n-side provides a voltage drop during the avalanche development due to the growing current and thus quenches the avalanche.

3. Measurement Setup

The measurements discussed here include current-voltage characteristics and studies of the SiPM response to low-intensity light. While results of the former measurements are mostly used to check the sample operability and to define the range of bias voltages for the latter studies, the measurements of the SiPM response to the light provide a number of parameters suitable for the comparison of different samples.

A principal scheme of the measurement setup is shown in fig. 2. The bias voltage and current through a SiPM sample are monitored in the voltage circuit. The SiPM is illuminated with light from a light emitting diode operated in a pulse mode. The signal from SiPM is read out with a charge-sensitive preamplifier and digitised with an integrating ADC. The LED pulse of about 6 ns duration and ADC gate of about 100 ns width are synchronised by means of a common trigger.

The measurements are done at room temperature. Temperature variation during the measurements done for one sample did not exceed 2°C, for all measurements discussed here the total variation was less than 4°C.

4. Measurement Results

Five samples of silicon photomultipliers have been studied. CPTA [1] produced samples distributed by Obninsk University and Forimtech [2], HAMAMATSU produced Multi-Pixel Photon Counter

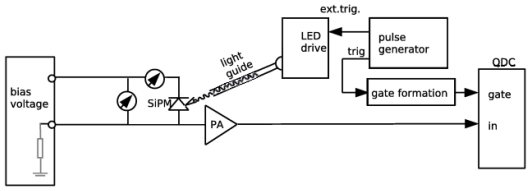

Fig. 2. A principal scheme of the measurement setup. The bias voltage and current through a SiPM sample are monitored in the voltage circuit. The SiPM is illuminated with light from a light emitting diode (LED) operated in a pulse mode. The signal from SiPM is read out with a charge-sensitive preamplifier (PA) and digitised with an integrating ADC. The LED pulse and ADC gate are synchronised by means of a common trigger.

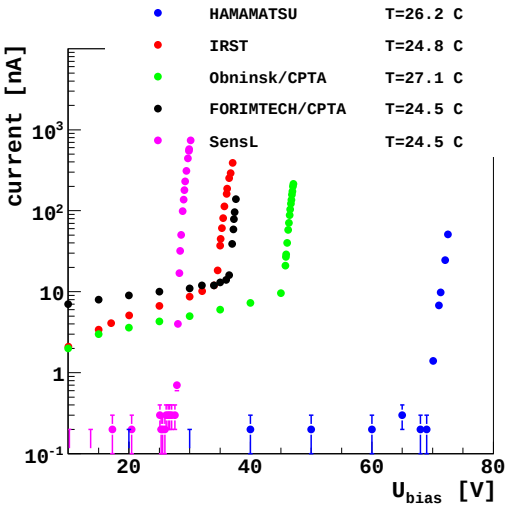

Fig. 3. The current-voltage characteristics measured for the studied samples.

S10362-11-025C [3], ITC-irst [3] and SensL [4] produced samples were compared on the base of the measurement results.

Fig. 3 shows the current-voltage characteristics measured for the listed samples.

Fig. 4 shows an example of the SiPM response to low-intensity light measured with the described setup. The peaked structure indicates the number of cells fired during one light pulse, starting with the pedestal for no cells fired. The distance between peaks corresponds to the SiPM gain.

The spectrum is fitted as a sum of gaussian distributions:

[1] CPTA, Russia, http://www.zao-cpta.ru
[2] Forimtech SA, http://www.forimtech.ch
[3] ITC-irst, Italy, http://www.itc.it/irst
[4] SensL,Ireland, http://www.sensl.com

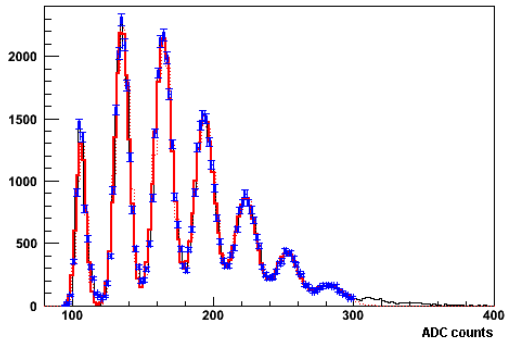

Fig. 4. ADC spectrum of the SiPM response to the low-intensity pulsed light (black) fitted to a superposition of seven gaussian peaks (red line).

$$\sum_i G(N_i, \mu_i, \sigma_i) = \sum_i G(N_i, \mu_0 + i \cdot g, \sigma_i), \qquad (1)$$

where μ_0 corresponds to the pedestal position and g is gain in units of ADC counts. From statistical considerations the width of i^{th} peak σ_i can be expressed as

$$\sigma_i = \sqrt{\sigma_0^2 + i \cdot \langle\sigma_{px}\rangle^2}, \qquad (2)$$

where σ_0 is the pedestal width and $\langle\sigma_{px}\rangle$ represents fluctuations of the one-cell response averaged over the active area of the sample.

In order to check reproducibility of the measurements and fitting procedures, a series of spectra was taken for the same bias voltage but under different light intensities. Fig. 5 shows the fitted width of i^{th} peak as a function of the peak number obtained from different measurements (top) and the corresponding averaged values (bottom). The bottom plot is fitted according to eq. 2.

The gain as a function of the overvoltage $U_{bias} - U_{brd}$ was studied for several values of the bias voltage. The breakdown voltage U_{brd} is defined here as the bias voltage corresponding to the gain equal to one. Fig. 6 shows the results obtained for the measured samples.

Fig. 7 shows gain normalised to the corresponding values of pedestal width (left) and $\langle\sigma_{px}\rangle$ (right) as functions of the overvoltage. Being averaged over the active area of SiPM, $\langle\sigma_{px}\rangle$ contains statistical and systematic parts:

$$\langle\sigma_{px}\rangle \sim \sqrt{N + \sigma_{nu}^2}, \qquad (3)$$

where N is the average number of charge carriers in the avalanche and σ_{nu} represents non-uniformity of the amplification over the SiPM active area. Since gain $g \sim N$, the ratio $g/\langle\sigma_{px}\rangle$ shown in fig. 7 (right)

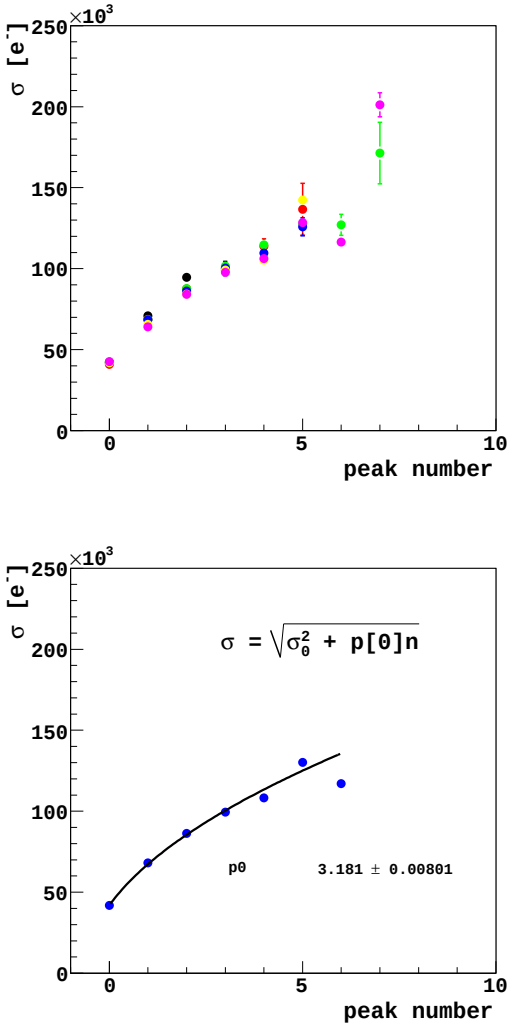

Fig. 5. Fit values for the width of i^{th} peak as a function of the peak number (top). The results obtained from different measurements are shown in different colours. The corresponding averaged values as a function of the peak number (bottom) are fitted according to eq. 2.

tends to a linear behaviour for the low gain values $N << \sigma_{nu}^2$. For the high gain values $N >> \sigma_{nu}^2$ the dependence would correspond to square root low $g/\langle\sigma_{px}\rangle \sim \sqrt{N}$ in the case of a constant σ_{nu}. As seen from fig. 7 (right) ratio $g/\langle\sigma_{px}\rangle \sim \sqrt{N}$ obtained for some of samples indicate growth of the non-uniformity factor σ_{nu} with the bias voltage.

5. Conclusion

The obtained results demonstrated operability and potential of the developed setup. Further de-

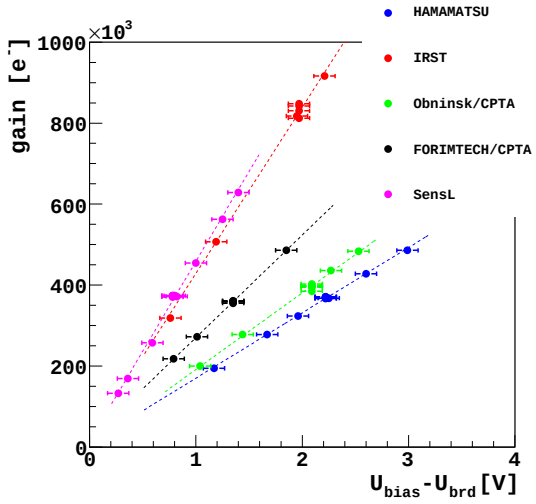

Fig. 6. Gain as a function of the overvoltage.

velopment and tune of the setup, measurement procedure and data treatment will allow to obtain comparative characteristics of diverse types of silicon photomultipliers.

6. Acknowledgements

We would like to thank Prof. R.Battiston (University and INFN of Perugia), Prof. V. Saveliev (Obninsk State University and DESY), Dr. I. Polak (Institute of Physics of the ASCR, Prague) and Mr. N. D'Ascenzo for support and fruitful discussions.

References

[1] G. Bondarenko, et al., Limited geiger-mode silicon photodiode with very high gain, Nucl. Phys. Proc. Suppl. 61B (1998) 347–352.
[2] P. Buzhan, et al., Silicon photomultiplier and its possible applications, Nucl. Instrum. Meth. A504 (2003) 48–52.
[3] H. P. K.K, Product catalogue no. kapd0002e02 (2007).

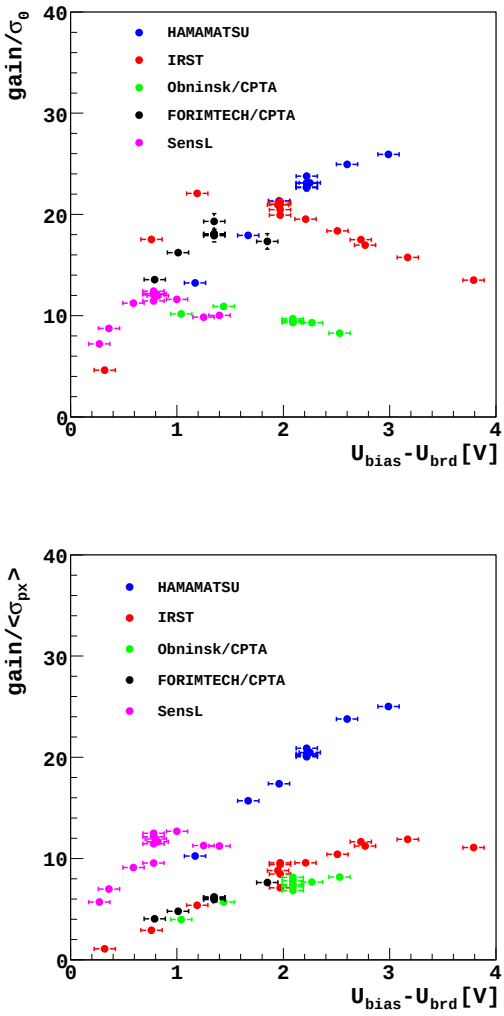

Fig. 7. The gain normalised to the corresponding values of pedestal width (left) and $\langle\sigma_{px}\rangle$ (right) as functions of the overvoltage.